

## Supporting Information

### Spectroelectrochemical Study of the AMP-Ag<sup>+</sup> and ATP-Ag<sup>+</sup> Complexes through Silver Mesh Electrode

FatoTano Patrice, Li-Jun Zhao, Essy Kouadio Fodjo, Da-Wei Li,\* and Yi-Tao Long\*

Key Laboratory for Advanced Materials, Shanghai Key Laboratory of Functional Materials Chemistry, School of Chemistry and Molecular Engineering, East China University of Science and Technology, 130 Meilong Road, Shanghai 200237, China.

\*Corresponding authors. \*E-mail: [ytlong@ecust.edu.cn](mailto:ytlong@ecust.edu.cn). Tel/Fax: 86-21-64252339.

\*E-mail: [ldwqiq@gmail.com](mailto:ldwqiq@gmail.com); Tel/Fax 86-21-64252339

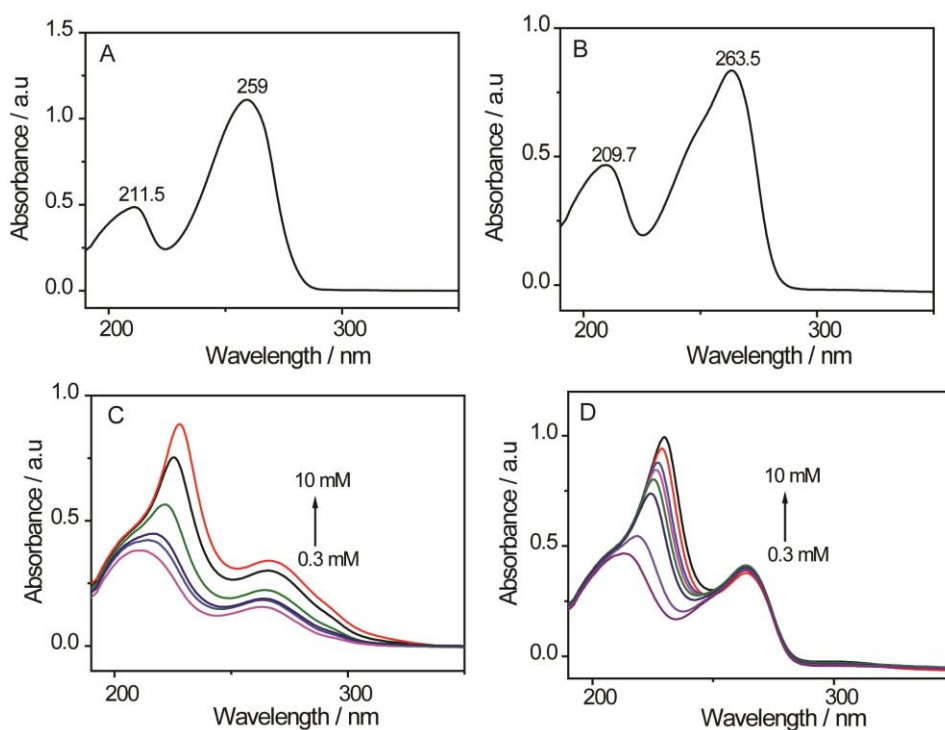
#### Contents

<b>1. Reaction with silver nitrate.....</b>	<b>S2</b>
<b>1.1. Reaction between adenine or 6-chloropurine riboside and silver nitrate.....</b>	<b>S2</b>
<b>1.2. Reaction between AMP or ATP and silver nitrate.....</b>	<b>S3</b>
<b>2. Spectroelectrochemical study.....</b>	<b>S3</b>
<b>2.1. Absorption spectrum observation of silver mesh.....</b>	<b>S3</b>
<b>2.2. Reaction between adenine or CPR and silver mesh in acetate buffer.....</b>	<b>S4</b>
<b>2.3. Reaction between AMP and silver mesh in acetate buffer at negative potential.....</b>	<b>S5</b>
<b>3. In-situ SERS study.....</b>	<b>S5</b>
<b>4. Electrochemical study using silver disk.....</b>	<b>S7</b>
<b>5. References.....</b>	<b>S8</b>

## 1. Reaction with silver nitrate

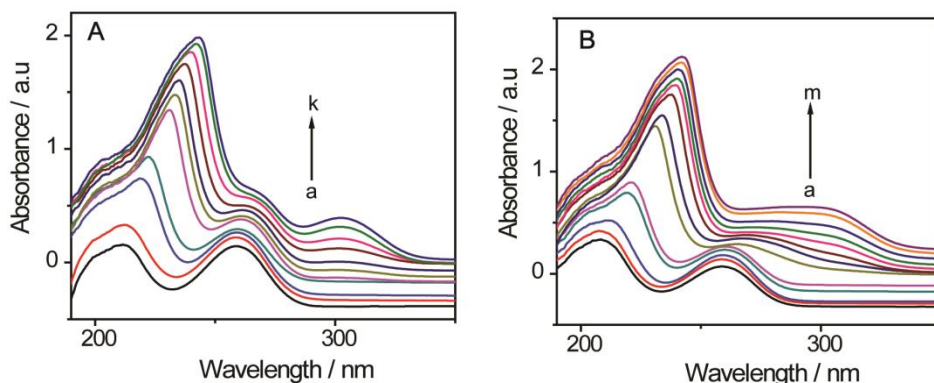
### 1.1. Reaction between adenine or 6-chloropurine riboside and silver nitrate

Fig. S1 displays the UV spectra of adenine and 6-chloropurine riboside (CPR) in water solvent. Both molecules show similar behavior upon addition of  $\text{AgNO}_3$ . Without  $\text{AgNO}_3$  in the solvent, their UV spectra indicate two well-defined peaks due to the aromatic ring portion (peak around 260 nm) and its residue (peak centered on 210 nm) as can be seen in Fig. S1A and S1B. In the presence of  $\text{AgNO}_3$  and by increasing its concentration, a hypochromic is observed in the region of 260 nm, while a red shift and a gradual increase in the absorbance intensity are observed at the peak with lower wavelength in their different spectra (Fig. S1C and S1D). Therefore, the interaction sites of  $\text{Ag}^+$ -adenine and  $\text{Ag}^+$ -CPR complexes formation are N-1, N-3, N-7, and particularly N-9 atom for adenine.<sup>1</sup>



**Fig. S1:** UV-vis spectra in deionized water of A) 0.3 mM adenine, B) 0.3 mM 6-chloropurine riboside (CPR), C)  $\text{Ag}^+$ /adenine complex using 0.3 mM adenine upon addition of  $\text{AgNO}_3$  solution (0.3, 0.6, 0.8, 2, 4, and 10 mM), and D)  $\text{Ag}^+$ /AMP complex using 0.3 mM adenine upon addition of  $\text{AgNO}_3$  solution (0.3, 0.5, 0.8, 1, 2, 4, 8, and 10 mM). The inset in A and B are the molecular structure of adenine and CPR, respectively.

## 1.2. Reaction between AMP or ATP and silver nitrate



**Fig. S2:** UV-vis spectra in deionized water of A)  $\text{Ag}^+/\text{AMP}$  complex using 0.4 mM AMP upon addition of  $\text{AgNO}_3$  solution (a – k: 0.4, 0.8, 2, 8, 10, 40, 60, 80, 100, 200 and 500 mM) and B)  $\text{Ag}^+/\text{AMP}$  complex using 0.3 mM AMP upon addition of  $\text{AgNO}_3$  solution (a – i: 0.3, 0.6, 0.8, 1, 4, 15, 20, 40, 80, 100, 200, 400, and 600 mM).

## 2. Spectroelectrochemical study

### 2.1. Absorption spectrum observation of silver mesh

To understand the behavior of silver mesh electrode in a buffer solution, its spectroelectrochemistry was carried out. Thus, the UV-vis spectra of silver mesh electrode in 0.2 M  $\text{CH}_3\text{COONa}-\text{CH}_3\text{COOH}$  at potential 500 mV at different times are evaluated as shown in Figure S3. From this Figure, one can clearly observe an enhancement in the absorbance intensity when the time increases. Besides, there is no obvious peak shift during the 45 initial minutes, while from 60 s to 300 s, a slight red shift from 232 to 233 nm is observed in the spectra due to the  $\pi \rightarrow \pi^*$  electronic transitions. These results prove the relative stability of the silver mesh electrode.

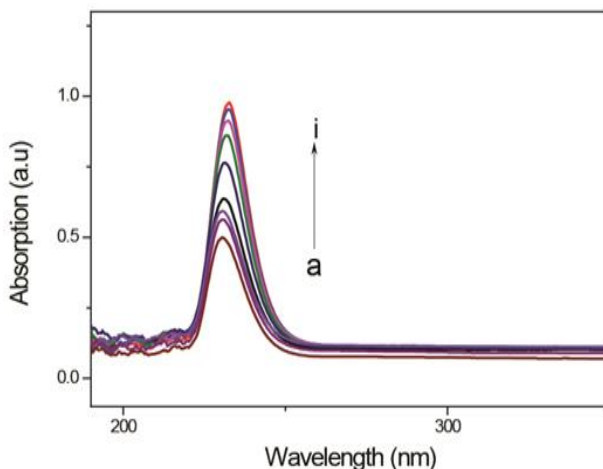


**Fig. S3:** UV-vis spectra of silver mesh in 0.2 M  $\text{CH}_3\text{COONa}-\text{CH}_3\text{COOH}$  (pH 6.0) at potential 0.5 V and different times a) 0 s , b) 5 s , c) 10 s , d) 30 s , e) 45 s , f) 60s , g) 120 s , h) 180 s , and i) 300 s .

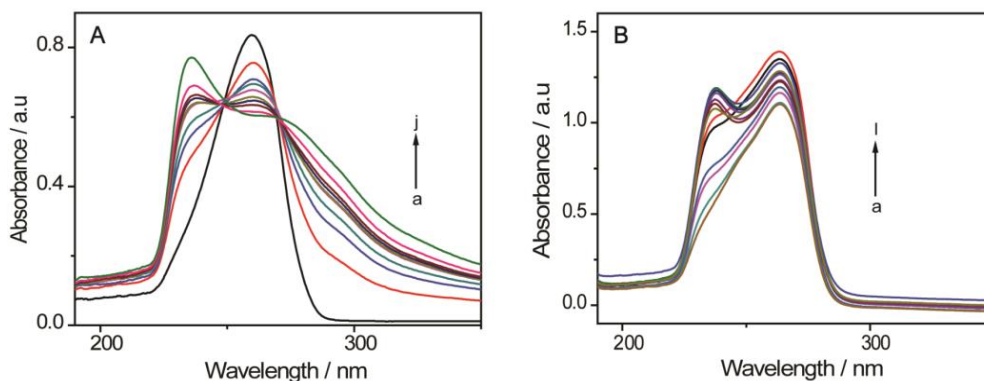
## 2.2. Reaction between adenine or CPR and silver mesh in acetate buffer

Figure S4 depicts the UV spectroelectrochemical study of adenine (0.3 mM) and 6-chloropurine riboside (CPR) (0.3 mM) on silver mesh electrode in 0.2 M CH<sub>3</sub>COONa-CH<sub>3</sub>COOH (pH 6.0) at 500 mV vs. Ag/AgCl. In figure S4A, one can observe an isosbestic point at 249 nm, which is due to the redox reaction of Ag oxidation, and another one at 270 nm that is related to the Ag<sup>+</sup>-adenine complex. Those isosbestic points are expressed by the equations 1 and 2, respectively.



where HX represents the nucleotide (AMP or ATP), a and b are the stoichiometric coefficients.

Albeit an increase in the peak intensity was observed beyond 310 nm, there was no peak at this wavelength, which shows that the coordination of Ag<sup>+</sup> ion does not happen on phosphate group but on nitrogen atoms.<sup>2-4</sup>



**Fig. S4:** UV-vis spectra of A) 0.3 mM adenine and B) 0.3 mM 6-chloropurine riboside on the silver mesh in 0.2 M CH<sub>3</sub>COONa-CH<sub>3</sub>COOH (pH 6.0) at 500 mV vs. Ag/AgCl.

### 2.3. Reaction between AMP and silver mesh in acetate buffer at negative potential

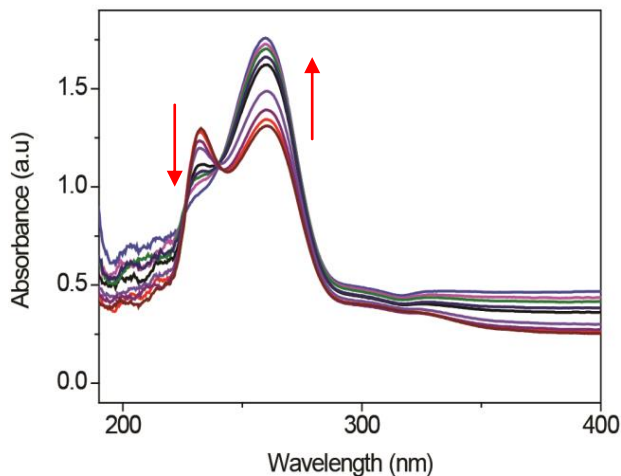


**Fig. S5:** UV-vis spectra of AMP on the silver mesh in 0.2 M  $\text{CH}_3\text{COONa}$ - $\text{CH}_3\text{COOH}$  (pH 6.0) at -500 mV vs. Ag/AgCl.

### 3. In-situ SERS analysis

It is well-known that Raman spectroscopy provides any information of molecules namely surface information and molecular structures. Fig. S6 shows the Raman spectra of AMP and ATP in acetate buffer solution containing silver mesh (Fig. a & b) and the Raman spectra of AMP and ATP powders (Fig. c & d). Additionally, to understand the different coordination occurred, we tabulated Raman frequencies with assignments of each adenine nucleotide to facilitate the interpretations (Tables 1 and 2).

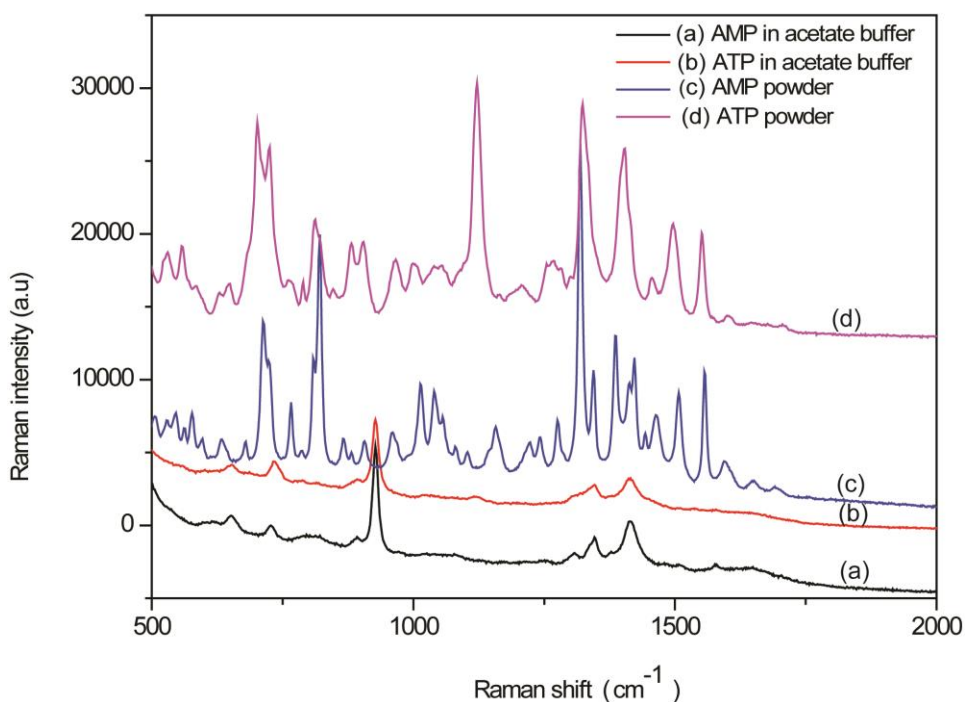


**Fig. S6:** Raman spectra of a) AMP and b) ATP in 0.2 M acetate buffer solution (pH 6.0) containing silver mesh. Raman spectra of c) AMP and d) ATP solids.

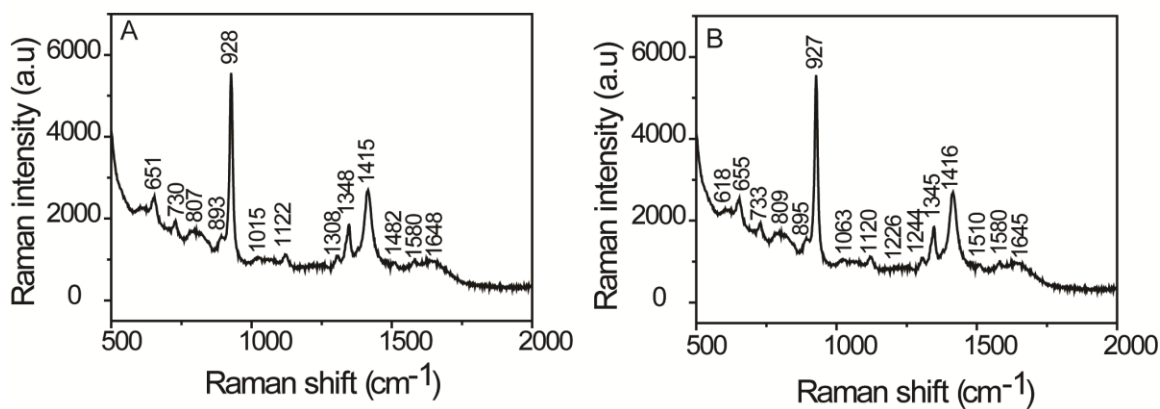


**Fig. S7:** Raman spectra of A) 40 mM ATP and B) 85 mM AMP in 0.2 M acetate buffer solution (pH 6.0) containing silver mesh electrode showing the different peak intensities.

Table S1: Assignment of the different peaks in Raman spectrum of ATP in acetate buffer (Figure 3A, spectrum h).  $\nu$  indicates stretching,  $\delta$  denotes bending,  $\tau$  shows wagging.

Frequencies (ATP)	assignment	references
651	$\tau(\text{C}_5\text{N}_7\text{C}_8)$	5
730	stretching in phase for bonds in adenine ring	6
807	$\nu(\text{O} - \text{P} - \text{O})$	7
893	$\nu(\text{N}_7\text{C}_8\text{N}_9), \nu(\text{C}_4\text{N}_9\text{C}_8), \nu(\text{C}_5\text{N}_7\text{C}_8)$	8
928	five-membered ring	5
1015	$\nu(\text{C}_4\text{N}_9), \nu(\text{N}_7\text{C}_8)$	9
1122	$\nu(\text{O} - \text{P} - \text{O})$	6
1348	$\nu(\text{C}_8\text{N}_9), \nu(\text{N}_3\text{C}_2), \delta(\text{C}_8\text{H}), \delta(\text{C}_2\text{H})$	8
1415	$\nu(\text{N}_7\text{C}_8), \nu(\text{C}_6\text{N})$	6
1484	$\nu(\text{C}_2\text{N}_3)$	10
1580	$\nu(\text{C}_4\text{C}_5), \nu(\text{N}_3\text{C}_4)$	6

Table S2: Assignment of the different peaks in Raman spectrum of AMP in acetate buffer (Figure 3B, spectrum f).  $\nu$  indicates stretching,  $\delta$  denotes bending,  $\tau$  shows wagging.

Frequencies (AMP)	assignment	references
534	$\nu(\text{N}_1\text{C}_6\text{C}_5), \nu(\text{C}_6\text{N})$	8
570	out-of-plane adenine breathing mode	5
618	$\nu(\text{C}_6\text{C}_5), \nu(\text{C}_6\text{N})$	8
655	$\tau(\text{C}_5\text{N}_7\text{C}_8)$	5
733	stretching in phase for all bonds in adenine ring	6
786	out-plane five and six-membered ring	11
809	$\nu(\text{O} - \text{P} - \text{O})$	6
895	$\nu(\text{N}_7\text{C}_8\text{N}_9), \nu(\text{C}_4\text{N}_9\text{C}_8), \nu(\text{C}_5\text{N}_7\text{C}_8)$	8
927	five-membered ring	5
978	$\nu(\text{O} - \text{P} - \text{O})$	12
1063	$\nu(\text{N}_9\text{C}_8), \delta(\text{N}_9\text{H})$	5
1075	$\nu(\text{N}_7\text{C}_8)$	12
1082	$\nu(\text{O} - \text{P} - \text{O})$	13
1226	$\nu(\text{O} - \text{P} - \text{O})$	6
1244	$\nu(\text{N}_7\text{C}_8), \nu(\text{N}_3\text{C}_2)$	8
1345	$\nu(\text{C}_8\text{N}_9), \nu(\text{C}_2\text{N}_3), \nu(\text{N}_7\text{C}_8)$	9
1374	ribose vibration	14
1416	$\nu(\text{N}_7\text{C}_8), \nu(\text{C}_6\text{N})$	6
1580	$\nu(\text{C}_4\text{C}_5), \nu(\text{N}_3\text{C}_4)$	6

#### 4. Electrochemical study using silver disk

The electrochemical behavior of AMP and ATP in 0.2 M  $\text{CH}_3\text{COOH}-\text{CH}_3\text{CHOONa}$  (pH 7.0) was explored using a silver disk by means of cyclic voltammetry. Fig. S7 shows the CV of the blank acetate buffer and acetate buffer containing 10 mM AMP (or ATP) at a scan rate of  $100 \text{ mV s}^{-1}$  in the potential range from 0.0 to 0.4 V and are depicted in Figures S2A, S2B, and S2C, respectively. As can be observed in these figures, the CVs of

the blank acetate buffer, AMP, and ATP within the buffer solution present a single irreversible reduction peak at 0.33 V, 0.21 V, and 0.22 V, respectively showing an irreversible process. This observation is due to the oxidation of the substance reduction product<sup>15</sup>.

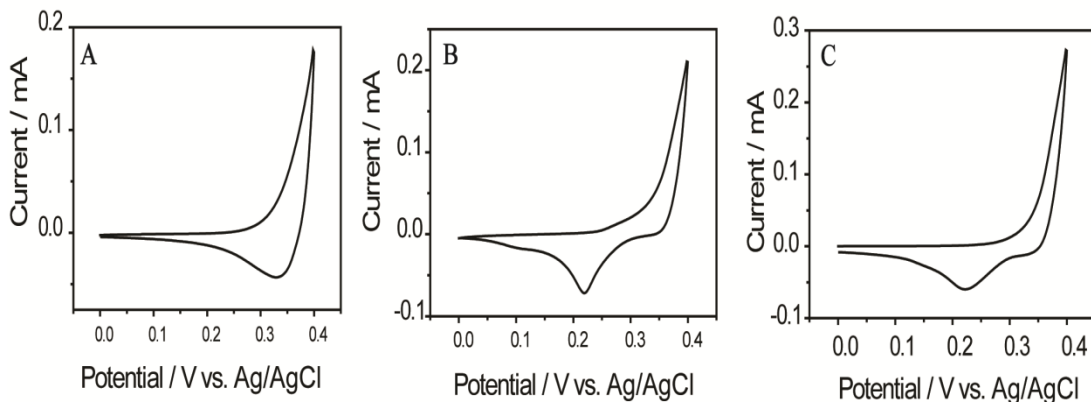


**Fig. S8:** CVs from silver disk in A) acetate buffer solution, acetate buffer solution containing B) 10 mM AMP and C) 10 mM ATP. The scan rate was 100 mV s<sup>-1</sup>.

## 5. References

- 1 E. Papadopoulou and S. E. J. Bell, *Analyst*, 2010, **135**, 3034.
- 2 C. Otto, 2008, **22**, 791–796.
- 3 C. Otto, F. M. de Mul, A. Huizinga and J. Greve, *J. Phys. Chem.*, 1988, **92**, 1626–310.
- 4 S. K. Kim, T. H. Joo, S. W. Suh and M. S. Kim, *J. Raman Spectrosc.*, 1986, **17**, 381–386.
- 5 B. Giese and D. McNaughton, *J. Phys. Chem. B*, 2002, **106**, 101–112.
- 6 R. Huang, H. T. Yang, L. Cui, D. Y. Wu, B. Ren and Z. Q. Tian, *J. Phys. Chem. C*, 2013, **117**, 23730–23737.
- 7 G. Forrest and R. C. Lord, *J. Raman Spectrosc.*, 1977, **6**, 32–37.
- 8
- 9 L. Chinsky, P. Y. Turpin and M. Duquesne, *Biopolymers*, 1963, **17**, 1347–1359.
- 10 V. Zhelyaskov and K. T. Yue, *Biochem. J.*, 1992, **287** (Pt 2), 561–6.
- 11 R. Santamaria, E. Charro, a Zacaras and M. Castro, *J. Comput. Chem.*, 1999, **20**, 511–530.
- 12 R. Huang, L. Bin Zhao, D. Y. Wu and Z. Q. Tian, *J. Phys. Chem. C*, 2011, **115**, 13739–13750.
- 13 L. Rimai, T. Cole, J. L. Parsons, J. T. Hickmott and E. B. Carew, *Biophys. J.*, 1969, **9**, 320–329.
- 14 R. Jastrzab, Z. Hnatejko, T. Runka, A. Odani and L. Lomozik, *New J. Chem.*, 2011, **35**, 1672.
- 15 E. Palecek and M. Bartosik, *Chem. Rev.*, 2012, **112**, 3427–3481.